OPTOELECTRONICS AND ADVANCED MATERIALS – RAPID COMMUNICATIONS Vol. 9, No. 9-10, September – October 2015, p. 1251 - 1259

Performance analysis & comparative study of uniform, apodized and pi-phase shifted FBGs for array of high performance temperature sensors

HANAN M. EL-GAMMAL, HEBA A. FAYED, AHMED ABD EL-AZIZ, MOUSTAFA H. ALY[#,*]
Photonic Research Lab (PRL), Electronics and Communications Engineering Department, College of Engineering and Technology, Arab Academy for Science, Technology and Maritime Transport, Alexandria, Egypt
[#] *Member of OSA*

In this paper, Theoretical analysis and numerical simulations are carried out to evaluate the performance of Different FBG types including Uniform, pi-phase shifted (πFBG) and various profiles Apodized FBGs for Temperature Sensing. The comparison and evaluation are done under a number of controlled parameters including grating length (L) and refractive index modulation amplitude (Δn_{ac}). Various evaluation techniques are used like Reflectivity, Side Lobes Analysis - including Side Lobes Strength, Side Lobe Suppression Ratio (SLSR), Difference between Main Lobe & Side Lobe and Number of observed Side lobes - Full Width at Half Maximum (FWHM), Roll-off Rate and Ripple Factor for judging the sensitivity and targeting an optimum performance of the temperature sensors. Our Analysis and comparison revealed that the uniform FBGs have three important areas that require improvement for temperature detection: Bandwidth, Sensitivity& Number of Harmonics (Side Lobes). This Problem is vanished when using pi-phase shifted FBG (πFBG) which recorded optimum results in terms of the introduced evaluation techniques. Also Nuttall & Proposed ($\cos^8$) Apodized FBGs showed remarkable results in suppressing the side lobes but on the expense of decreasing the peak reflectivity. A simple experimental design of temperature sensor was also introduced in this paper.Finally, it was concluded that uniform FBG can't be used as efficient temperature array sensor but πFBG can be used instead.

(Received June 2, 2015; accepted September 9, 2015)

Keywords: Fiber Bragg Grating (FBG), Uniform, Apodized, pi-phase shifted FBG (πFBG), Array of fiber-optic Sensors, Temperature Sensors, Ultrasonic Detection

1. Introduction

Recently, Fiber-Optic Sensors became an emerging technique for temperature & strain detections and measurements. The main reason for this is that the Fiber-Optic sensors possess many advantages over their Electronic counterparts because they are made up of durable non-conductive silica glass making them immune to electromagnetic interference, their light weight, small size, intrinsically safe, corrosion resistant and has a small profile [1]. Owing to their excellent multiplexing capability, sensors based on Fiber Bragg Grating (FBG) are particularly attractive for applications where a large number of sensors are desired such as industrial process control, fire detection systems, temperature profiling in electrical power transforms [2,3] since a FBG sensor occupies only a very narrow bandwidth, a distributed sensor array could be easily fabricated by writing many FBG sensors onto a single fiber at different locations [4]. Also FBG sensors are intra-core fiber element and are wavelengths encoded, thus eliminating the amplitude or intensity variation problem existing in other Fiber-Optic sensors [5].

Using Array of FBGs Temperature sensors make it easier for spectral information to be demultiplexed allowing the value of each FBG temperature to be extracted as a function of position along the length of the fiber. In addition to that they operate over a wide range of temperatures and re ideal for remote measuring. [6]

The Mechanism of detection for a FBG in most applications relies on observing a shift in its reflection spectrum. But the traditional FBGs (uniform) have two important areas that require some improvement for detection: **Sensitivity & Bandwidth**. Short wavelength shifts resulting from low amplitude sensors emission resulting in limited sensitivity of traditional FBG sensor and the width of the typical FBG reflection spectrum is approximately 0.3 nm which leads to shallow spectral slopes.

So thesolution was to use π-Phase-shifted Fiber Bragg Gratings (πFBG) by introducing a π-Phase-shift discontinuity at the center of the grating (separating a FBG into two separate smaller FBGs resulting in an extremely narrow notch forming in the center of the reflection spectrum) and due to the phase discontinuity, a πFBG can be conceptually considered to be a Fabry–Perot cavity formed by two FBG mirrors.

For efficient and highly sensitive temperature sensor, it is desired to have high Peak Reflectivity (stronger reflectivity), Narrow bandwidth or Full Width at Half Maximum (FWHM), high Side Lobe Suppression Ration (SLSR), high Roll-off rate (Side lobe Asymptotic Decay),

high Ripple factor andSmall number &amplitude of side lobes (side lobes strength).

A uniform FBG bandwidth and reflectivity depend on grating length (L) and grating strength (Δn_{ac}) but the side lobes strength and number can't be controlled, that's why we introduced the Apodization which offer significant improvement in side-lobe suppression but on the expense of reducing the peak reflectivity. [8]

In this work, we demonstrated the effect of different Apodization profiles (Gaussian, Hamming, Barthan, Nuttall, Tanh, Sinc, Raised Sine and Proposed ($\cos^8$)), which were previously studied in [8] in addition to pi-phase shifted FBG (πFBG) on temperature sensor FBG-based.

The simulations in this paper were done by the use of the following software programs: Matlab (version 2009a), OptiSystem (version 7) and OptiGrating (version 4.2.2).

This paper is organized as follows: Section 2 isfor the theory and modeling, followed by temperature sensor simulation setup in Section 3. Section 4 is devoted for the results and discussion. Finally, the conclusion of the paper is provided in Section 5.

2. Theory and modeling

2.1 Uniform FBG

The forward propagated light is reflected at Bragg wavelength:

$$\lambda_B = 2n\Lambda \tag{1}$$

Where$\lambda_B$is the Bragg wavelength (wavelength of the reflection peak amplitude), n is the effective refractive index of optical mode propagating along the fiber and Λis the period of FBG structure.

For a uniform Bragg grating formed within the core of an optical fiber with an average refractive index n_0. The index of the refractive profile can be expressed as: [9]

$$n(z) = n_0 + \Delta n \cos(\frac{2\pi z}{\Lambda}) \tag{2}$$

Where Δn is the amplitude of the induced refractive index perturbation, ʌ is the nominal grating period and z is the distance along the fiber longitudinal axis.

Using coupled-mode theory the reflectivity of a grating with constant modulation amplitude and period is given by the following expression: [10]

$$R(l,\lambda) = \frac{\kappa^2 sinh^2(sl)}{\Delta\beta^2 sinh^2(sl) + s^2 cosh^2(sl)} \tag{3}$$

Where $R(l,\lambda)$ is the reflectivity, which is a function of the grating length l and wavelength λ, $\Delta\beta = \beta - \pi/\Lambda$is the detuningwave vector, $\beta = 2\pi n_0/\lambda$is the propagation constant and $s^2 = \kappa^2 - \Delta\beta^2$ and $\kappa = \frac{\pi\Delta n}{\lambda} M_{power}$isac coupling coefficient, $M_{power}$is the fraction of the fiber mode power contained by the fiber core.

In the case where the grating is uniformly written through the core, M_{power}can be approximated by $1 - V^{-2}$, where $V = \frac{2\pi}{\lambda} a\sqrt{n_{co}^2 - n_{cl}^2}$is the normalized frequency of the fiber, a is the core radius,$n_{co}$and $n_{cl}$are the core and cladding indices respectively. At the center wavelength of the Bragg grating the wave vector detuning is $\Delta\beta = 0$, therefore the expression for the reflectivity becomes:

$$R(l,\lambda) = tanh^2(\kappa l) \tag{4}$$

The reflectivity increases as the induced index of refraction change gets larger. Similarly, as the length of the grating increases, so does the resultant reflectivity.

2.2 pi-phase shifted FBG (πFBG)

π-Phase-shifted Fiber Bragg Gratings (πFBG) differs from a traditional FBG by introducing a π-Phase-shift discontinuity at the center of the grating thus separating a FBG into two separate smaller FBGs (see Fig. 1(a)) resulting in an extremely narrow notch forming in the center of the reflection spectrum (see Fig. 1(b)) which can be used to facilitate sensor detection in a similar manner to normal FBGs by locking the laser wavelength to the linear region of the spectral notch and observing the change in reflectivity due to the spectral shift. [7] Due to the phase discontinuity, a πFBG can be conceptually considered to be a Fabry–Perot cavity formed by two FBG mirrors. When the two FBGs are highly reflective, the quality factor of the Fabry–Perot cavity is increased, leading to an extremely narrow spectral notch for highly sensitive detection [12].

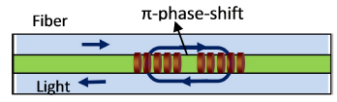

(a)

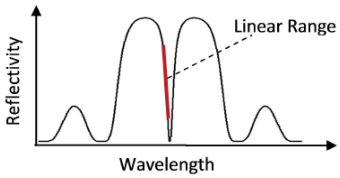

(b)

Fig. 1. (a) Schematic of πFBG (b) Schematic of Reflection spectrum of πFBG

2.3 Apodized FBG

Apodized FBG offer significant improvement in side-lobe suppression but on the expense of reducing the peak reflectivity.

Apodized gratings have variations along the fiber in the refractive index modulation envelope (Δn_{ac}) with constant grating period and constant DC refractive index function.

The index of the refractive profile of Apodized can be expressed as: [11]

$$n(z) = n_{co} + \Delta n_o A(z)\, n_d(z) \tag{5}$$

Where n_{co} is the core refractive index, Δn_o is the maximum index variation, $n_d(z)$ is the index variation function and $A(z)$ is the Apodization function.

Apodization profiles are:

1- Uniform:

$$A(z) = 1,\ 0 \le z \le L \tag{6}$$

2- Gaussian Function:

$$A(z) = \exp(-ln2(\frac{2(z-\frac{L}{2})}{0.5\,L})^2),\ 0 \le z \le L \tag{7}$$

3- Hamming Function:

$$A(z) = 0.54 - 0.46\cos(\frac{2\pi z}{L}),\ 0 \le z \le L \tag{8}$$

4- Barthan Function:

$$A(z) = 0.62 - 0.48\left|\frac{z}{L} - 0.5\right| + 0.38\cos(\frac{z}{L} - 0.5),\ 0 \le z \le L \tag{9}$$

5- Nuttall Function:

$$A(z) = 0.3635819 - 0.48917755\left(2\pi\frac{z}{L}\right) + 0.1365996\left(4\pi\frac{z}{L}\right) - 0.0106411\left(6\pi\frac{z}{L}\right),\ 0 \le z \le L \tag{10}$$

6- Tanh Function:

$$A(z) = \tanh\left(4\frac{z}{L}\right) * \tanh\left(4\frac{1-z}{L}\right), 0 \le z \le L \tag{11}$$

7- Sinc Function:

$$A(z) = \mathrm{sinc}\left(2\pi\frac{z-L/2}{L}\right),\ 0 \le z \le L \tag{12}$$

8- Raised Sine Function:

$$A(z) = \left(\sin\left(\frac{z}{L}\right)\right)^2, 0 \le z \le L \tag{13}$$

9- Proposed ($\cos^8$) Function: [8]

$$A(z) = \left(\cos\left(\frac{2z}{L} - 1\right)\right)^8, 0 \le z \le L \tag{14}$$

2.4 Temperature & pressure sensing

Fiber Bragg Grating sensors are developed for quasi-distributed or multi-point (strain, temperature, pressure etc.) monitoring in both surface mounted and embedded sensing applications to provide local damage. The phase-matching condition of the fiber grating determines the Bragg resonance wavelength, λ_B, and the basic principle of an FBG based sensor system lies in the monitoring of the wavelength shift of the returned Bragg-signal, as a function of the measurand (environmental factors or physical disturbance).

The wavelength shift $\Delta\lambda_B$ of a fiber Bragg grating sensor subject to physical disturbance (temperature and strain) can be expressed as: [13]

$$\frac{\Delta\lambda_B}{\lambda_B} = (1 - \rho_e)\varepsilon + (\alpha + \zeta)\Delta T \tag{15}$$

Where $\Delta\lambda_B$ is the wavelength shift, λ_B is the initial wavelength, ρ_e is photo-elastic (or strain-optic) constant, ε is axial strain (or change in strain), α is thermal expansion coefficient, ζ is thermo-optic coefficient and ΔT is temperature change.

For the Temperature Sensing;when a fiber Bragg grating is subject to a temperature variation, two phenomenon's entail a variation $\Delta\lambda_B$ of the characteristic wavelength.

Due to thermal expansion of the fiber material and the temperature dependence of the refractive index.

$$\frac{\Delta\lambda_B}{\lambda_B} = (\frac{1}{\Lambda}\frac{d\Lambda}{dt} + \frac{1}{n}\frac{dn}{dt})\Delta T \tag{16}$$

Where $\alpha = \frac{1}{\Lambda}\frac{d\Lambda}{dt}$ is the thermal expansion coefficient and $\zeta = \frac{1}{n}\frac{dn}{dt}$ represents thermo-optic coefficient.

It was found that there is a linear relation between shifts in wavelength and Temperature (see Fig 2).

The typical temperature sensitivity of a fiber Bragg grating at 1550 nm is 10.4 pm/°C.[14]

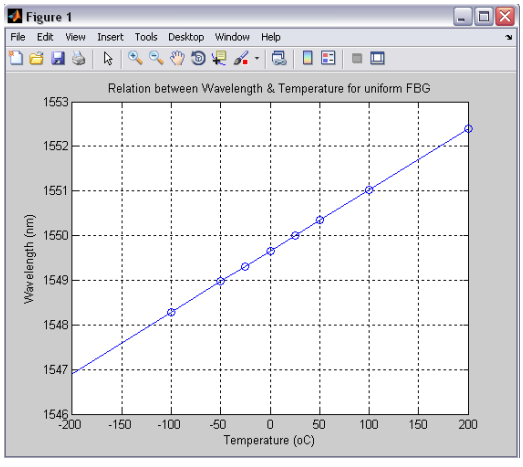

Fig. 2. Simulated spectrum of linear relation between shifts in wavelength vs temperature for uniform FBG

3. Temperature sensor simulation setup

Fig. 3 represents the Block Diagram of a simple experimental setup of temperature sensor system using a

uniform FBG (this simulation was made by the use of OptiSystem Software program, version 7).

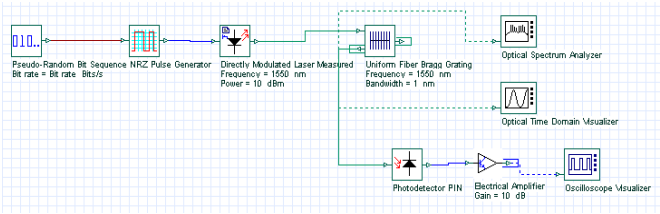

Fig. 3. Block Diagram of Temperature Sensor System setup using uniform FBG

The system consists of the following:

1-Pseudo-Random bit Sequence Generator: generates random sequence of bits with rate = 1 Gb/s.

2- NRZ Pulse Generator: generates Non-Return to Zero rectangular pulse signals from pseudo random sequence.

3- Directly Modulated Laser Measured: a transducer which converts the pulse signals from the electrical domain to the optical domain. It is a narrow line-width laser source which generates a laser beam from the pulse signals with Wavelength = 1550 nm and Power = 10 dB_m.

4- Uniform FBG: on which the temperature changes are applied (sensor). Detection is done here by locking laser to the linear region of the reflection spectrum and observing the shift in the wavelength λ_B.

5- Optical Spectrum Analyzer: displays the optical signal power in the frequency domain (Power vs frequency (Hz) or Wavelength (m)).

6- Optical Time Domain Visualizer: displays the optical signal power in the time domain (Power vs Time (s)).

7- Photo-detector PIN: converts the signal from the optical domain to the electrical domain.

8- Electrical Amplifier: amplifies the electrical signal for later display by Gain = 10 dB.

9- Oscilloscope Visualizer: displays the signal amplitude in the electrical domain (Amplitude (a.u.) vs Time (s)).

4. Results & discussion

4.1 Parameters definition

Now we will analyze and compare the performance of Uniform, pi-phase shifted (πFBG)and Apodized FBGs (Gaussian, Hamming, Barthan, Nuttall, Tanh, Sinc, Raised Sine and Proposed ($\cos^8$)) targeting the optimum type of FBG that can be used as a temperature sensor based on its performance.

The following simulations are performed for step index, single mode fiber, Fiber Bragg Grating (FBG) with core radius (r_{co}) = 2 μm, core refractive index (n_{co}) = 1.447, cladding radius (r_{cl}) = 8 μm, cladding refractive index (n_c) = 1.444 and Bragg or center wavelength (λ_B) = 1550 nm (1.55 μm).

Refractive index modulation change (Δn_{ac}) varies from $0.5*10^{-4}$ (weak grating) to $5*10^{-4}$ (strong grating) while Grating Length (L) is maintained at 10000 μm (10 mm). Then, the simulations are repeated with varying L from 10,000 (short grating) to 90,000 μm (long grating) while maintaining Δn_{ac} at $4*10^{-4}$.

In order to compare different FBG profiles: Uniform, different Apodization profiles (Gaussian, Barthan, Hamming, Nuttall, Raised Sine, Sinc, Tanh and Proposed ($\cos^8$)) and pi-Phase shifted FBGs, the

Δn_{ac} = $4*10^{-4}$and L = 10000 μm (10 mm) are kept constant.

The Evaluation Parameters are:

1- Trasmittivity: Ratio of Transmitted (Forward-carrier) Power to the input power: $T = \frac{P_F}{P_{IN}}$ and for spectrum calculations the transmission is obtained at the end of the device: $T = \frac{P_B}{P_{IN(\lambda)}}$, z = end of device and $\lambda \in (\lambda_{min}, \lambda_{max})$ where P_B is the backward power, P_F is the forward power and P_{IN} is the input power.
(*units: dB or % or a.u*).

2- Reflectivity: Ratio of Reflected (back-reflected) Power to the input power: $R = \frac{P_B}{P_{IN}}$ and for spectrum calculations the reflection is obtained at the end of the device: $R = \frac{P_B}{P_{IN(\lambda)}}$, $z = 0$ and $\lambda \in (\lambda_{min}, \lambda_{max})$.
(*units: dB or % or a.u*).

Peak Reflectivity: Maximum Reflected Power at the center wavelength λ_B.

3- FWHM (Full Width at Half Maximum):Width of the signal at 50% (half) of the maximum power amplitude (*units: μm*). [15]

A general expression of the approximate FWHM of the grating is: $\Delta\lambda = \lambda_B s \sqrt{(\frac{\Delta n_{ac}}{2n_{eff}})^2 + (\frac{1}{N})^2}$ (15)

Where λ_B is the Bragg (center) wavelength, s is a parameter indicting the strength of the gratings (~1 for strong gratings and ~0.5 for weak gratings), N is the number of grating planes, Δn_{ac} is the change in the refractive index and n_{eff} is the effective refractive index.

4- Side Lobes Analysis:

a- Maximum Left / Right Side Lobe Strength: Amplitude of First Left / Right Reflections appearing off-resonance (at wavelengths other that center wavelength λ_B) at both sides of the Main Lobe (*units: dB*).

b- SLSR (Side Lobe Suppression Ratio): Ratio between the first and last side lobes indications the slope by which the side lobes are suppressed or decayed (*units: %*).

c- Difference between the main and first side lobe: measuring the difference in amplitudes between peak reflected power and first left / right side lobe (*units: dB*).

d- Number of Side Lobes: Counting the number of harmonics or reflections on both left and right sides of the main lobe located at the center wavelength λ_B.

e- Side Lobe Asymptotic Decay (Roll-off rate): Ratio between the decay of the side lobes (difference between first and last side lobes) and the covered wavelengths (*units: dB/μm*).

It is desired to have high Peak Reflectivity (stronger reflectivity), high SLSR, high Roll-off rate (Side lobe Asymptotic Decay), Reducing the number, amplitude of side lobes (side lobes strength) and FWHM (narrower bandwidth).

4.2 Performance Analysis of Uniform FBG based on varying L & Δn_{ac}

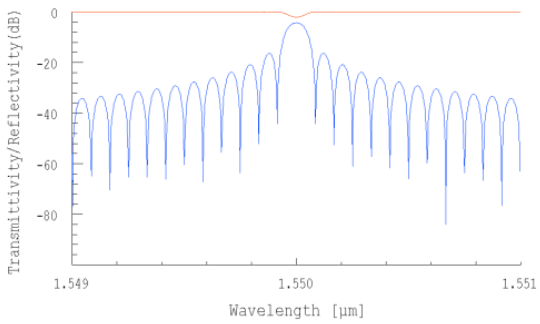

Fig. 4.Transmittivity/Reflectivity (dB) vs Wavelength (µm) for uniform FBG (L=10000 µm and $\Delta n_{ac}=4*10^{-4}$)

Fig. 4 presents the Transmission & Reflection Spectrums (Relation between Transmittivity/Reflectivity (dB) and Wavelength (µm)) of a uniform FBG at L=10000µm and $\Delta n_{ac}=4*10^{-4}$.

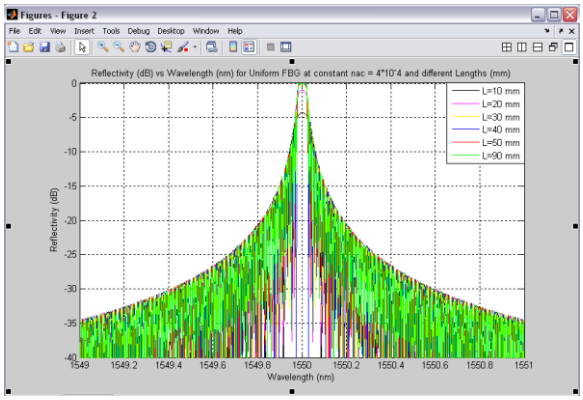

Fig. 5. Reflectivity (dB) vs Wavelength (nm) for uniform FBG (at constant $\Delta n_{ac}=4*10^{-4}$) and different L (mm)

Fig. 5 presents the reflection spectrum of uniform FBG at constant $\Delta n_{ac}=4*10^{-4}$ and varying L (10, 20, 30, 40, 50, 90 mm). From which, it can be observed that Increasing L (the longer the grating):

- Increases the Peak Reflectivity (increased from -4.28222 to -0.0592176 dB for L=10,000 and 40,000 µm respectively) which is desirable.
- Increases Side Lobes Strength or Amplitude of First Side Lobe (increased from -20.8402 to -5.658832 for L=10,000 and 40,000 µm respectively) which is not desirable.
- Decreases FWHM (decreased from $1.976*10^{-3}$ to $1.968*10^{-3}$µm for L=10,000 and 40,000 µm respectively) which is desirable.
- Decreases SLSR (decreased from 47.86199397% to 18.57643369% for L=10,000 and 40,000 µm respectively) which is not desirable.
- Decreases Difference between the main and first side lobe (decreased from 12.12568 to 5.687116 dB for L=10,000 and 40,000 µm respectively) which is not desirable.
- Increases Number of side lobes (increased from 11 to 47 for L=10,000 and 40,000 µm respectively) which is not desirable.
- Increases Roll-off rate or Side lobe Asymptotic Decay (increased from $-2.125989209*10^{4}$ to $-2.184689017*10^{4}$ dB/ µm for L=10,000 and 40,000 µm respectively) which is desirable.

Thus the longer the grating the higher the peak reflectivity (see Fig. 6), the higher the Roll-off rate and the narrower the bandwidth which is required. But on the other hand, making the grating longer increases the number, strength of side lobes and SLSR which is not required.

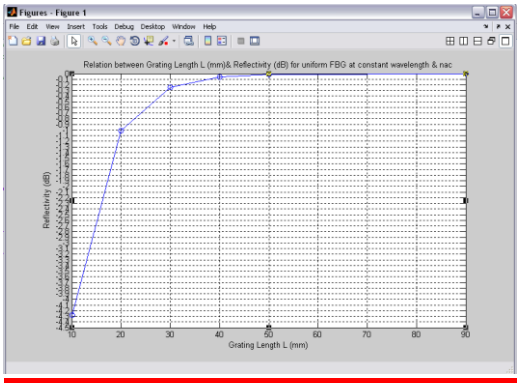

Fig. 6. Grating Length L (mm) vs Reflectivity (dB) at constant wavelength λ = 1550 nm and $\Delta n_{ac}=4*10^{-4}$

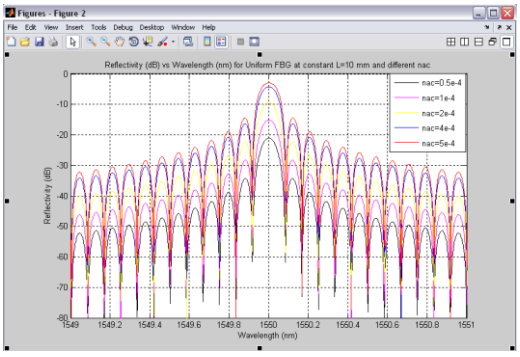

Fig. 7. Reflectivity (dB) vs Wavelength (nm) for uniform FBG (at constant L=10 mm) and different Δn_{ac}

Fig. 7 presents the reflection spectrum of uniform FBG at constant L=10 mm and varying Δn_{ac} (0.5, 1, 2, 4, $5*10^{-4}$). It can be observed that Increasing Δn_{ac} (the stronger the grating):

- Increases the Peak Reflectivity (increased from -15.1045 to -4.28222 dB for L=10,000 and 40,000 µm respectively) which is desirable.
- Increases Side Lobes Strength or Amplitude of First Side Lobe (increased from -28.2865 to -20.8402 dB for $\Delta n_{ac} = 1*10^{-4}$ and $4*10^{-4}$ respectively) which is not desirable.
- Increases FWHM (Increased from $1.969*10^{-3}$ to $1.978*10^{-3}$µm for $\Delta n_{ac} = 1*10^{-4}$ and $4*10^{-4}$ respectively) which is not desirable.
- Decreases SLSR (decreased from 69.64391215% to 47.86199397% for $\Delta n_{ac} = 1*10^{-4}$ and $4*10^{-4}$ respectively) which is not desirable.
- Decreases Difference between the main and first side lobe but not very much (decreased from 13.182 to 12.12568 dB for $\Delta n_{ac} = 1*10^{-4}$ and $4*10^{-4}$ respectively) which is not desirable.
- Number of side lobes is maintained (11 for both $\Delta n_{ac} = 1*10^{-4}$ and $4*10^{-4}$) which is desirable.
- Decreases Roll-off rate or Side lobe Asymptotic Decay (decreased from $-2.149304556*10^{4}$ to $-2.125989209*10^{4}$ dB/ µm for $\Delta n_{ac} = 1*10^{-4}$ and $4*10^{-4}$ respectively) which is not desirable.

Thus the stronger the grating the higher the peak reflectivity (see Fig. 8) and the number of side lobes is kept constant which is required. But on the other hand, making the grating stronger decreases the Roll-off rate, increases the strength of side lobes, SLSR, bandwidth which is not required.

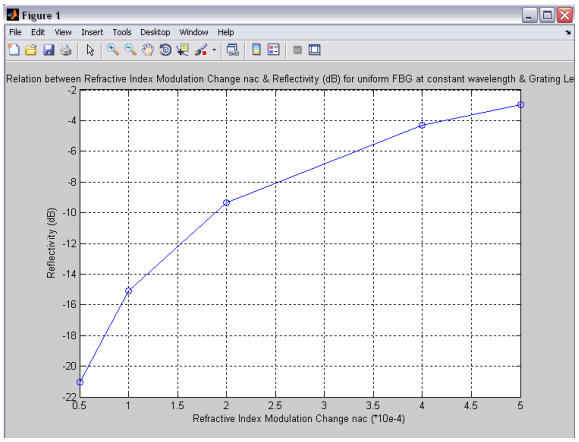

Fig. 8. Refractive index Modulation change (Δn_{ac}) vs Reflectivity (dB) at constant wavelength λ = 1550 nm and L=10mm

4.3 Performance Analysis of πFBG based on varying L & Δn_{ac}

Fig. 9 presents the Transmission & Reflection Spectrums of a πFBG at L=10000µm and $\Delta n_{ac}=4*10^{-4}$. From which it can be observed that now we separated the FBG into two separate smaller FBGs separated by a very narrow notch in the center of the reflection spectrum to improve sensitivity & reduce bandwidth. Also when compared to uniform FBG under the same parameters (see Fig. 4), the Reflectivity increased (approaching to 0 dB) and the side lobes are greatly reduced.

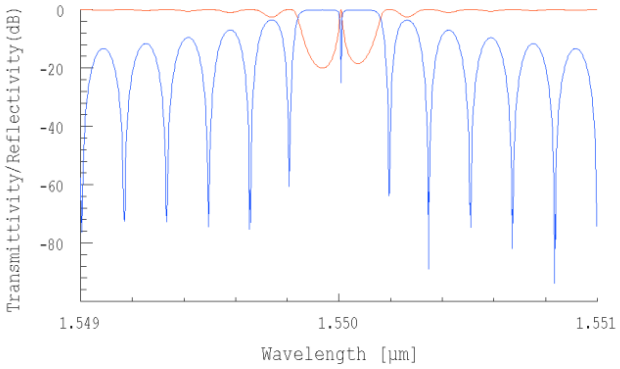

Fig. 9. Transmittivity/Reflectivity (dB) vs Wavelength (µm) for πFBG at L = 10000 µm and $\Delta n_{ac} = 4*10^{-4}$

4.4 Comparing the performance analysis of uniform, Apodized and πFBGs at constant L=10000µm and $\Delta n_{ac}=4*10^{-4}$

Fig. 10 presents the reflection spectrum of uniform, 8 Apodized FBGs (Gaussian, Hamming, Barthan, Nuttall, Tanh, Sinc, Raised Sine and Proposed ($\cos^8$)) and πFBG at constant $\Delta n_{ac}=4*10^{-4}$ and L=10000µm.

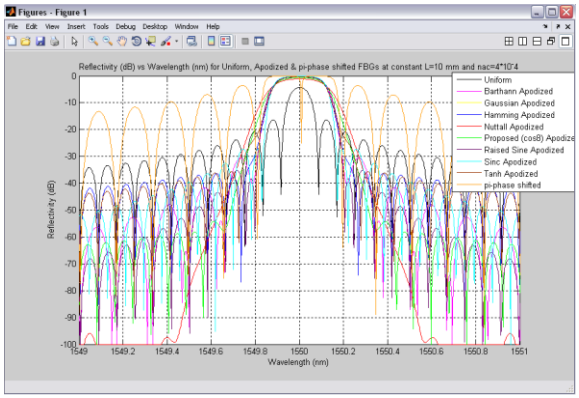

Fig. 10. Reflectivity (dB) vs Wavelength (nm) for Uniform, Apodized & pi-phase shifted FBG (at constant L=10 mm and $\Delta n_{ac}=4*10^{-4}$)

The results of this Fig. are summarized in Table 1.

Table 1. Apodization Profiles Evaluation Summary (underlined = best reading)

Type of FBG	Peak Reflectivity (dB)	SL Strength (dB)		FWHM ($*10^{-3}$µm)	SLSR (%)	Diff. bet. ML & SL (dB)	No. of SL	Roll-off Rate ($*10^4$dB/µm)	Ripple Factor
		Left	Right						
1- Uniform	-4.28	-20.84	-16.34	1.98	47.86	12.13	11	-2.13	-0.91
2- Gaussian	-0.32	-35.61	-35.62	1.93	88.21	30.53	9	-1.23	-0.99
3- Barthan	-0.38	-41.60	-41.61	1.85	82.16	30.24	9	-3.92	-0.99
4- Hamming	-0.28	-36.38	-36.39	1.93	90.54	30.75	9	-0.62	-0.99
5- Nuttall	-1.08	-95.98	-95.99	0.848	100.00	96.45	2	0.43	-0.98
6- Raised Sine	-0.38	-35.26	-35.26	1.26	57.98	30.80	10	-2.87	-0.99
7- Sinc	-0.19	-27.28	-27.28	1.93	52.48	20.72	10.5	-2.52	-0.96
8- Tanh	-0.32	-35.61	-35.62	1.93	88.22	30.53	9	-1.25	-0.99
9- Proposed (cos^8)	-0.66	-58.11	-58.11	0.97	92.62	50.36	8	-1.48	-0.98
10- πFBG	-0.04 -0.07	-3.53	-3.61	1.98	31.88	-3.55	5	-1.48	-1.00
BEST	10	5	5	5	5	5	5	3	10

From Table 1 we can observe the following:

- In terms of Peak Reflectivity the πFBG has recorded the highest with 2 peaks: -0.0432916 and -0.06440764 dB (99% and 98.53% respectively). While Nuttall has recorded the lowest peak reflectivity of -1.08489 dB (77.9%). It is also recognized that the uniform has recorded the second best peak reflectivity after the πFBG compared to other apodized FBGs which suppress the side lobes on the extent of reducing the peak reflectivity.
- In terms of Side Lobes Strength the Nuttall has recorded the lowest side lobes of amplitudes -95.9783 dB (left) and -95.9864 dB (right), followed by the Proposed (cos^8) in the second place of amplitudes -58.107 dB (left) and -58.1103 dB (right). But unfortunately the πFBG recorded the highest side lobes of amplitudes -3.52797 dB (left) and -3.61308 (right).
- In terms of FWHM the Nuttall FBG has recorded the lowest bandwidth of amplitude 0.848 nm followed by the Proposed (cos^8) of amplitude 0.966 nm. But unfortunately πFBG recorded the widest bandwidth of amplitude 1.978 nm *(but if we considered that πFBG has two peaks and we get the bandwidth of one of them that would result in narrow bandwidth of 0.989 nm)*
- In terms of SLSR the Nuttall has recorded the highest with ratio 100.0000417% followed by the Proposed (cos^8) with ratio 92.61578228%. But unfortunately the πFBG recorded the lowest ratio of 31.88361265%.
- In terms of Difference between Main Lobe and First Side Lobe the Nuttall has recorded the highest difference of 96.44758 dB followed by the Proposed (cos^8) of difference 50.355144 dB. But unfortunately the πFBG recorded the least difference between amplitudes of Main Lobe and First Side Lobe of -3.545913.
- In terms of Number of Side Lobes the Nuttall has recorded the least number of 2 side lobes followed by the πFBG of 5 side lobes. While the uniform has recorded the highest number of side lobes of 11 (main problem of uniform FBG which is being solved by introducing the apodization filters).
- In terms of Roll-off Rate (Side lobes Asymptotic Decay) the Barthan has recorded the highest rate of -3.919592705*10^4 dB/µm followed by the Raised Sine with rate -2.866054918*10^4 dB/µm. But unfortunately the Nuttall recorded the lowest roll-off rate of 0.4324772727*10^4 dB/ µm. Meanwhile the πFBG recorded a good roll-off rate of -.1.477184299*10^4 dB/ µm.
- In terms of Ripple factor the πFBG has recorded the highest amplitude of -0.99907736 followed by the Sinc with amplitude of -0.99677038. While the uniform has recorded the lowest ripple factor of amplitude -0.90295707.

  From the previous results and notes we can deduce that although πFBG has the peak reflectivity, ripple factor and good roll-off rate but unfortunately when talking about the side lobes analysis and FWHM it shows a remarkable failure. Meanwhile the Nuttall and Proposed (cos^8) apodized FBG solve this problem.

4.5 Effect of temperature variation on uniform FBG and a linearity check

Fig. 11 presents the Reflection Spectrum of a uniform FBG at L=10000 µm, $\Delta n_{ac}=4*10^{-4}$ and T=25°C (Room temperature) → Black colored, which is being heated to 50, 100 & 200°C and then cooled to 0, -25, -50, -100, -200°C to observe the wavelength shifts caused by this (Table 2 summarizes those results).

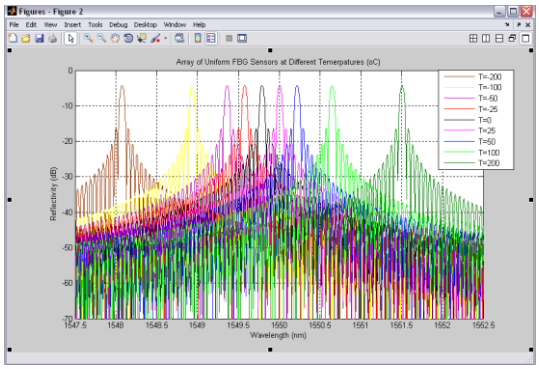

Fig. 11. Array of Uniform FBG sensors at different Temperatures (^0C) Ranging from -200 to 200^0C and at constant L = 10000 μm and $\Delta n_{ac} = 4*10^{-4}$

Table 2 Relation between Temperature (^0C) & Center Wavelength λ (nm) for uniform FBG at constant L = 10 mm and $\Delta n_{ac}=4*10^{-4}$

Temperature (^0C)	**Center Wavelength (nm)**
-200	1546.914
-100	1548.286
-50	1548.972
-25	1549.314
0	1549.658
25 (Reference)	**1550**
50	1550.342
100	1551.028
200	1552.4

Since the good and efficient temperature sensor requireshigh reflectivity, low sidelobes and narrow FWHM (usually 0.4 nmwide) to obtain high sensitivity. In addition to, steep roll-off to reject adjacent channels and stable operation over increased temperature.

From Table 2 and Fig. 11 we can conclude that uniform FBG is not an optimum solution for temperature sensor array because of its high sidelobes, broad FWHM and (larger than required value) although it has a good roll-off rate and stable over increased temperature (see Fig. 12). And from our previous results we can deduce that πFBG solved all those problems and can be used as efficient temperature sensors array.

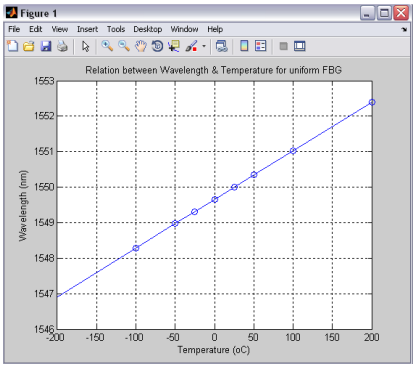

Fig. 12. Linear relation between Temperature (^0C) &Wavelength (nm) for Uniform FBG at constant L = 10000 μm and $\Delta n_{ac} = 4*10^{-4}$

5. Conclusion

In this paper, Performance of Uniform, pi-phase shifted (πFBG)and various profiles Apodized FBGs has been analyzed and compared under control of changing the grating length (L) and refractive index

modulation amplitude (Δn_{ac})targeting the optimum type of FBG that can be used as a temperature sensor based on its performance.

Based on our analysis, results showed that for any type of FBG longing the grating length–increasing L– results in higher peak reflectivity, higher Roll-off rate and narrower bandwidth (FWHM) which is desirable,on the expense of increasing the number, strength of side lobes and SLSR which is not desirable.

On the other hand, making the gratings stronger – increasing Δn_{ac}– results in higher peak reflectivity and keeps the number of side lobes constant which is desirable, on the expense of decreasing the Roll-off rate, increasing strength of side lobes, SLSR and bandwidth which is not desirable.

While maintaining constant L=10000μm and $\Delta n_{ac}=4*10^{-4}$ to compare different types of FBGs; results showed that although*πFBG*showed an outstanding performance when compared to uniform, withthe highest 2peak reflectivitiesand the highest ripple factorbut unfortunately when talking about the side lobes analysis and FWHM it shows a remarkable failure(*but if we considered one of the peaks ofπFBG, itsbandwidth will be narrow of 0.989 nm*). Meanwhile the Nuttall and Proposed ($\cos^8$) apodized FBGs can solve this problem with the lowest side lobes strength, narrowestFWHM, highest SLSR, less number of side lobes. On the other hand the Barthann Apodized has recorded the highest Roll-off Rate (Side lobes Asymptotic Decay) followed by Raised Sine Apodized and also πFBGrecorded a good roll-off rate.

Finally, it was concluded that uniform FBG can't be used as efficient temperature array sensor but πFBG can be used instead.

References

[1] S. Kreger, S. Calvert, E. Udd, in 15th Opt. FiberSensors Conf. Tech. Dig., **1**, 355 (2002).
[2] Qi Zhang, Nan Liu, Thomas Fink, Hong Li, Wei Peng, Ming Han, IEEE photonics technology letters, **24**(17), (2012).
[3] G. C. Righini, World Scientific, 2009.
[4] Thomas Fink, Electrical Engineering Theses and Dissertations, Paper 44, November 2012.
[5] H. Venghaus, Wavelength Filters in Fibre Optics1 (2006).
[6] G. J. de Villiers, J. Treurnicht, R. T. Dobson, Applied Thermal Engineering **38**, 143 (2012).
[7] Tongqing Liu, Ming Han, IEEE Sensors Journal, **12**(7), (2012).
[8] Nazmi A. Mohammed, Taha A. Ali, Moustafa H. Aly, Master of Science Thesis, AIP Advances **3**, 122125 (2013).

[9] Turan Erdogan, Journal of Lightwave Technology, **15**(8), (1997).
[10] Andreas Othonos, Kyriacos Kalli, David Pureur, Alain Mugnier, chapter 5, Publication Date: May 30, 1999, ISBN 10: 0890063443, ISBN-13: 978-0890063446.
[11] Sunita P. Ugale, V. Mishra, Special Issue of International Journal of Computer Applications on Electronics, Information and Communication Engineering - ICEICE No.3, Dec 2011.
[12] M. LeBlanc, et al., Opt. Lett., **24**(16), 1091 (1999).
[13] Andreas Othonos, Kyriacos Kalli, David Pureur, Alain Mugnier, chapter 5, Publication Date: May 30, 1999, ISBN-10: 0890063443, ISBN-13: 978-089006344.
[14] Harmanpreet Kaur, Ritika Dhiman, Amandeep Kaur, International Journal of Engineering Research and Technology, ISSN 0974-3154, **3**(3), 357 (2010).
[15] T. T. Tam, D. Q. Trung, T. A. Vu, L. H. Minh, D. N. Chung, VNU Journal of Science Mathematics-Physics **23**, 237 (2007).
[16] V. M. Sunita P. Ugale, IJCA Special Issue On Electronics, Information and Communication Engineering ICEICE(3), December 2011.

*Corresponding author: drmosaly@gmail.com